Acta Pharmacologica Sinica

www.nature.com/aps

ARTICLE

Mzb1 protects against myocardial infarction injury in mice via modulating mitochondrial function and alleviating inflammation

Lu Zhang[1,2], Yi-ning Wang[1,2], Jia-ming Ju[2], Azaliia Shabanova[1,2,3], Yue Li[1,2], Ruo-nan Fang[1,2], Jia-bin Sun[1,2], Ying-ying Guo[1,2], Tong-zhu Jin[1,2], Yan-yan Liu[1,2], Tian-yu Li[1,2], Hong-li Shan[1,2,4], Hai-hai Liang[1,2,4] and Bao-feng Yang[1,2,4]

Myocardial infarction (MI) leads to the loss of cardiomyocytes, left ventricle dilation and cardiac dysfunction, eventually developing into heart failure. Mzb1 (Marginal zone B and B1 cell specific protein 1) is a B-cell-specific and endoplasmic reticulum-localized protein. Mzb1 is an inflammation-associated factor that participates a series of inflammatory processes, including chronic periodontitis and several cancers. In this study we investigated the role of Mzb1 in experimental models of MI. MI was induced in mice by ligation of the left descending anterior coronary artery, and in neonatal mouse ventricular cardiomyocytes (NMVCs) by H_2O_2 treatment in vitro. We showed that Mzb1 expression was markedly reduced in the border zone of the infarct myocardium of MI mice and in H_2O_2-treated NMVCs. In H_2O_2-treated cardiomyocytes, knockdown of Mzb1 decreased mitochondrial membrane potential, impaired mitochondrial function and promoted apoptosis. On contrary, overexpression of Mzb1 improved mitochondrial membrane potential, ATP levels and mitochondrial oxygen consumption rate (OCR), and inhibited apoptosis. Direct injection of lentiviral vector carrying Len-Mzb1 into the myocardial tissue significantly improved cardiac function and alleviated apoptosis in MI mice. We showed that Mzb1 overexpression significantly decreased the levels of Bax/Bcl-2 and cytochrome *c* and improved mitochondrial function in MI mice via activating the AMPK-PGC1α pathway. In addition, we demonstrated that Mzb1 recruited the macrophages and alleviated inflammation in MI mice. We conclude that Mzb1 is a crucial regulator of cardiomyocytes after MI by improving mitochondrial function and reducing inflammatory signaling pathways, implying a promising therapeutic target in ischemic cardiomyopathy.

Keywords: myocardial infarction; cardiomyocyte; Mzb1; mitochondria; inflammation; apoptosis; AMPK-PGC1α pathway; macrophages

Acta Pharmacologica Sinica (2021) 42:691–700; https://doi.org/10.1038/s41401-020-0489-0

INTRODUCTION

Acute myocardial infarction (AMI), one of the leading causes of morbidity and mortality worldwide, is characterized by blocked blood flow to the coronary arteries, resulting in various biochemical and metabolic alterations within the myocardium, including mitochondrial dysfunction and, if prolonged, the death of cardiomyocytes [1]. Despite the identification of many risk factors for AMI and elucidation of the underlying mechanisms, our understanding of the pathophysiological mechanisms of AMI is still incomplete, and clinical management of AMI remains imperfect.

Numerous endogenous factors contribute to AMI. These include the production of reactive oxygen species (ROS), changes in intracellular calcium and pH, and the triggering of inflammatory mechanisms, all of which interact to mediate opening of the mitochondrial permeability transition pore (PTP) [2], leading to eventual cardiomyocyte death [3]. In addition to the loss of physiological function, damaged mitochondria actively drive inflammatory responses [4]. It was reported that damaged mitochondria could promote the expression of NLRP3 [5]. Therefore, it is necessary to improve mitochondrial function and relieve inflammation after MI.

The *Mzb1* gene, which encodes a B-cell-specific and ER-localized protein [6], functions as a cochaperone of the substrate-specific chaperone GRP94 under ER stress conditions [7] and participates in the activation of integrin β1 [8]. Previously, research on the role of Mzb1 has focused on immune diseases, cancer, and chronic lymphocytic leukemia. However, whether Mzb1 plays an important role in other inflammatory diseases has been questioned. Once a patient has MI, the area of the infarct triggers a series of inflammatory responses. However, the role of Mzb1 in AMI has not yet been investigated. Many of the injuries resulting from AMI

[1]Department of Pharmacology (State-Province Key Laboratories of Biomedicine-Pharmaceutics of China, Key Laboratory of Cardiovascular Research, Ministry of Education), College of Pharmacy, Harbin Medical University, Harbin 150081, China; [2]Northern Translational Medicine Research and Cooperation Center, Heilongjiang Academy of Medical Sciences, Harbin Medical University, Harbin 150081, China; [3]Department of Outpatient and Emergency Pediatric, Bashkir State Medical University, Ground Floor, Teatralnaya Street, 2a, 450000 Ufa, Russia and [4]Research Unit of Noninfectious Chronic Diseases in Frigid Zone (2019RU070), Chinese Academy of Medical Sciences, Harbin 150081, China
Correspondence: Hai-hai Liang (lianghaihai@ems.hrbmu.edu.cn) or Bao-feng Yang (yangbf@ems.hrbmu.edu.cn)
These authors contributed equally: Lu Zhang, Yi-ning Wang, Jia-ming Ju

Received: 16 April 2020 Accepted: 20 July 2020
Published online: 5 August 2020

converge on the mitochondria, making it a fundamental organelle for studying this disease [9]. In our preliminary experiment, Mzb1 was also found to be localized to the mitochondria. We therefore hypothesized that Mzb1 plays a role in AMI by modulating mitochondrial function and oxidative stress.

Here, we showed that Mzb1 alleviated cardiomyocyte apoptosis and inflammation induced by MI and H_2O_2. More importantly, Mzb1 restored the ATP content, inhibited the production of ROS in cardiomyocytes by improving mitochondrial function, alleviated the release of cytokines, and recruited macrophages to the infarcted myocardium.

MATERIALS AND METHODS

Mouse model of MI

Male C57BL/6 mice (weighing 20–25 g, Liaoning Changsheng Biotechnology Co. LTD, Liaoning, China) underwent ligation of the left descending anterior coronary artery (LAD) to establish an MI model. The MI model was established with a procedure similar to that previously described in detail [10]. The use of mice in this study was approved by the Laboratory and Animal Care Committee of Harbin Medical University (Harbin, China). After 24 h of ligation, the hearts were rapidly removed and prepared for TTC (2,3,5-triphenyltetrazolium chloride) staining or other experimental interventions. All experiments were performed in accordance with the Guide for the Care and Use of Laboratory Animals published by the US National Institutes of Health (NIH Publication No. 85-23, revised 1996).

Isolation of primary NMVCs and treatment

Neonatal mouse ventricular cardiomyocytes (NMVCs) were dissociated from 1- to 3-day-old mice as described in our previous studies [11]. The cells were cultured in Dulbecco's modified Eagle's medium (DMEM) supplemented with 1% penicillin/streptomycin and 10% fetal bovine serum. Cultured primary NMVCs were transfected with plasmid (pLVX-mCMV-ZsGreen-mMzb1*Myc, pLVX-mCMV-ZsGreen) or siRNA (si-Mzb1)/NC (negative control) after 36 h of treatment with 200 μM H_2O_2 for another 12 h before measurements.

Cell culture

The Ana-1 (murine macrophage) cell line was purchased from Shanghai Enzyme Research Biotechnology Co., Ltd. (Shanghai, China). Ana-1 cells were cultured in 25-cm^2 cell culture flasks, 6-well plates, 12-well plates, or 24-well plates with DMEM (Biological Industries, Israel) supplemented with 10% fetal bovine serum (FBS; Biological Industries, Cromwell, CT, USA) and 1% penicillin/streptomycin (Beyotime Biotechnology, Shanghai, China). The cells were maintained at 37 °C with 5% CO_2 and 95% air. After starvation in serum-free medium for 12 h, the cells were transfected with plasmid or siRNA and prepared for the following experimental interventions.

Protein isolation and western blotting

Total proteins were extracted from cardiomyocytes and the infarction border zone of the mouse left ventricular wall. After transfection or other treatments, the cells were lysed with 30 μL of RIPA buffer (Roche Molecular Biochemicals, Basel, Switzerland), and protein concentrations were detected using a BCA kit (Beyotime Biotechnology, Shanghai, China) according to the manufacturer's guidelines. Protein samples (50–80 μg) were separated on SDS-PAGE gels and transferred to nitrocellulose membranes. After blocking the membranes with 5% skim milk in phosphate-buffered saline (PBS) for 1 h at room temperature, the membranes were probed with anti-Mzb1 (Abcam, Cambridge, MA, USA), anti-Bcl-2, anti-Bax, anti-Cytochrome *c*, anti-PGC1α, anti-β-actin (Proteintech, Wuhan, China), anti-p-AMPK (Beyotime Biotechnology, Shanghai, China), anti-NLRP3 and anti-CCL2 (Wanlei, Shenyang, China) antibodies at 4 °C overnight. The nitrocellulose membranes were washed with PBST (PBS containing 0.5% Tween 20) three times, followed by incubation with a fluorescence-labeled secondary antibody (IRDye700/800 mouse and rabbit antibodies) (Santa Cruz Biotechnology, Foster, California, USA). Protein levels were determined using Odyssey Clx (Gene Company Limited, Hong Kong, China), and the band intensities were quantified using Image Studio software.

Quantitative RT-PCR

RNA was isolated using TRIzol reagent according to the manufacturer's instructions. With 5× All-in-One Mastermix, RNA was reverse transcribed to complementary DNA (cDNA). Diluted cDNA was then subjected to real-time RT-PCR with gene-specific primers in the presence of SYBR Green by a 7500 Fast real-time PCR system. The mRNA levels of the different groups were normalized to those of the control group. The specific primers used in this study as follows:

IL-1β: forward, 5′-GAAATGCCACCTTTTGACAGTG-3′ and reverse, 5′-TGGATGCTCTCATCAGGACAG-3′; IL-6: forward, 5′-CACAGCAAGGCCTAGGAAAG-3′ and reverse, 5′-TTGGTTCAGCCACTGCCGTA-3′; TNFα: forward, 5′-TGGATGCTCTCATCAGGACAG-3′ and reverse, 5′-TGGATGCTCTCATCAGGACAG-3′; and Mzb1: forward, 5′-GCGAAAGCAGAGGCTAAATC-3′ and reverse, 5′-GGACCCCCAGAAATCATCA-3′.

TUNEL staining

Cells were fixed in 4% paraformaldehyde in PBS and permeabilized with 0.1% Triton X-100 in 0.1% sodium citrate. An in situ apoptotic cell death detection kit (fluorescein, Roche Applied Science) based on the TUNEL assay was used according to the manufacturer's instructions to detect apoptotic cells. Negative controls were included in each case by omitting the TUNEL enzyme terminal deoxynucleotidyl transferase reaction mixture and incubating the cells with the label solution. PBS containing 5 μg/mL 4′,6-diamidino-2-phenylindole (DAPI) was prepared to stain nuclei. The number of TUNEL-positive cells (green cells) and the total number of cells (blue cells) were determined.

Immunohistochemistry

The infarction border zone of the mouse left ventricular wall was fixed in 4% paraformaldehyde for 3 days and dehydrated for 24 h. Paraffin-embedded heart tissues were sliced into 5 μm sections. Immunohistochemical staining was performed using antibodies against Mzb1 and CD68. Quantification of the immuno-positive area was determined by ImageJ, and the results are indicated as the positive staining area/total area.

Measurement of intracellular ROS

NMVCs were incubated for 30 min with 10 μM 2′,7′-dichlorodihydrofluorescein diacetate (H2DCF-DA) probe, a fluorogenic dye used to measure ROS within cells. After fixation in 4% paraformaldehyde and washing with PBS 4 times, the cells were incubated in DAPI for 10 min to stain nuclei. The fluorescence signals were analyzed by a fluorescence microscope.

ATP determination

The level of ATP was measured by an ATP assay kit (Beyotime Biotechnology, Shanghai, China) based on a bioluminescence technique. Cells were washed once with PBS and transferred to lysis buffer. The supernatant was centrifuged at 12,000 × *g* for 5 min at 4 °C and mixed with ATP detection buffer before analysis by luminescence spectrometry. The final ATP content of each sample was normalized to its protein concentration measured by a BCA Protein Assay Kit (Beyotime Biotechnology, Shanghai, China).

Mitochondrial respiratory measurements

Whole-cell respiratory function was determined by high-resolution respirometry (Oxygraph-2k; Oroboros Instruments, Innsbruck, Austria) with procedures described in a previous study [12].

Briefly, the uncoupler (1 mM uncoupler: FCCP, niclosamide, and BAM15) was titrated in steps of 1 μL to a final concentration of 0.5 μM at intervals of 120 s until reaching the maximum noncoupled flux. Routine respiration (routine) was recorded after stabilization. Maximal mitochondrial respiration (MMR) in the mitochondria of NRVMs was calculated by subtracting the oxygen consumption rate (OCR) elicited by 2 μg/mL oligomycin from the maximum oxygen consumption rate induced by mitochondrial uncouplers. Reserve respiratory capacity (RRC) was equal to the difference between the maximum oxygen consumption rate and routine oxygen consumption rate. Inhibitors of complexes CI (rotenone, 0.5 μM) and CIII (antimycin A, 2.5 μM) were administered to assess the residual oxygen consumption.

To determine mitochondrial respiration, the number of cells was kept at $5 \times 10^5 \sim 10^6$ by cell counting in each group, and the initial respiratory value (routine value) for the control group was used as the standard to normalize other tested groups. The routine value of the control was set at 1. In each round of experiments, a control was set to account for the absence of a standard for normalization of the tested data.

Cell viability assay

Cell viability was measured by MTT assay. NMVCs were seeded in 96-well plates at a density of 5×10^3/well. After 48 h, the NMVCs were incubated in serum-free DMEM for 4 h. Transfection reagents and H_2O_2 were added to the cells. Then, the NMVCs were treated with 5 mg/mL MTT (20 μL/well) for 4 h. After the DMEM had been carefully removed, DMSO (150 μL/well) was added, followed by shaking for 15 min. The absorbance at 490 nm was measured using an Infinite 200 PRO microplate spectrophotometer (Tecan, Salzburg, Austria), and each measurement was obtained in triplicate. Relative absorbance values (normalized to the control) were used as an indication of cell viability.

Wound healing and transwell assays

For wound-healing assays, Ana-1 cells were seeded at a density of 1×10^6 cells/well in six-well plates. An artificial wound was created on the confluent cell monolayer after transfection using a sterile 10-μL pipette tip. The suspended cells were washed away with PBS, and the cells were then cultured in medium with 2% FBS (Biological Industries). The wounds were photographed with a light microscope at 48 h after treatment. In vitro cell migration was investigated using a 24-well insert Transwell apparatus (8.0 μm; Corning, NY, USA) in a migration assay. For the migration assay, 5×10^4 cells were suspended in 200 μL of serum-free DMEM and placed in the top chambers, and NMVCs were placed in the bottom chambers. Forty-eight hours after transfection, cells that had not penetrated through the membrane were removed with a cotton swab, while those adhered to the lower surface of the membrane were stained with a 0.1% crystal violet solution. The number of migrated cells in five randomly selected fields was counted under a light microscope (magnification ×200; Olympus, Tokyo, Japan).

Statistical analysis

All values are expressed as the mean ± SEM. Differences between two groups were determined by Student's *t*-test. A two-tailed P value < 0.05 indicated statistical significance. Data were analyzed using GraphPad Prism 6.0.

RESULTS

Downregulation of Mzb1 in the ischemic myocardium and H_2O_2-challenged cardiomyocytes

To explore the role of Mzb1 in AMI, the expression of Mzb1 was detected in MI mice 24 h after LAD ligation. As illustrated in Fig. 1a, b, the protein and mRNA levels of Mzb1 in the border zone of the infarct myocardium of MI mice were considerably lower than those in the equivalent area of animals in the Sham group. Qualitatively, the same results were observed with immunohistochemical staining for the Mzb1 protein (Fig. 1c). Similarly, Mzb1 was substantially downregulated at both the mRNA and protein levels in primary cultured NMVCs exposed to 200 μM H_2O_2 (Fig. 1d, e).

Cytoprotective effect of Mzb1 against H_2O_2-induced cardiomyocyte apoptosis

To elucidate the role of Mzb1 downregulation in MI, we assessed changes in cell viability after the artificial silencing of Mzb1 by siRNA (si-Mzb1). The efficacy of si-Mzb1 in silencing endogenous Mzb1 was confirmed by the marked knockdown of Mzb1 at both the protein (Fig. 2a) and mRNA (Fig. 2b) levels. As depicted in Fig. 2c, the viability of NMVCs was considerably decreased 12 h after H_2O_2 (200 μM) insult, and this change was markedly exacerbated by si-Mzb1. The TUNEL assay showed similar results and verified that the observed decrease in cell viability was primarily due to apoptotic cell death (Fig. 2d). To investigate whether this increase in apoptosis was attributable to the mitochondrial death pathway, we determined alterations in expression of the mitochondria-related factors Bax/Bcl-2 and Cyt-*c*. The Western blot results showed that the Bcl-2 protein level was decreased, whereas that of Bax was increased by si-Mzb1, resulting in a significant increase in the Bax/Bcl-2 ratio, and Cytochrome *c* (Cyt-c) expression was also upregulated after the silencing of Mzb1 (Fig. 2e).

Next, we tested the effects of Mzb1 overexpression on cardiomyocyte apoptosis. The Western blot results in Fig. 3a demonstrated that the transfection of pLVX plasmid carrying the Mzb1 gene (pLVX-mCMV-ZsGreen-mMzb1*Myc, Mzb1) remarkably increased the protein level of Mzb1, but transfection of empty plasmid (pLVX-mCMV-ZsGreen, pLVX) did not significantly alter Mzb1 expression. pLVX-Mzb1 effectively rescued the death of NMVCs induced by H_2O_2, as indicated by the increased cell viability after transfection of Mzb1 relative to transfection of pLVX in the presence of H_2O_2 (Fig. 3b). Moreover, the TUNEL assay showed that pLVX-Mzb1, but not pLVX, suppressed the apoptosis of NMVCs caused by H_2O_2 (Fig. 3c).

Mitochondria are susceptible to various cellular environmental cues and can activate the apoptotic pathway upon exposure to oxidative stress [13]. Abnormal upregulation of Bax and concomitant downregulation of Bcl-2, resulting in an increase in the Bax/Bcl-2 ratio, and the release of Cyt-*c* from mitochondria to the cytoplasm are key steps in activation of the mitochondrial death pathway. Our results showed that the protein level of Cyt-*c* and the Bax/Bcl-2 ratio was pronouncedly increased by H_2O_2 and that pLVX-Mzb1 abrogated these detrimental alterations, while pLVX failed to produce such beneficial effects (Fig. 3d).

Mzb1 improves mitochondrial function and decreases ROS production

Mitochondrial damage due to excess oxygen free radical production is believed to be the primary cause of cardiac cell death following ischemia injury or in response to cardiotoxic chemotherapy agents [14, 15]. Given that oxidative phosphorylation drives the synthesis of mitochondrial ATP, we investigated the potential role of Mzb1 in regulating mitochondrial respiration and mitochondrial ATP levels.

We first observed that exposure of NMVCs to 200 μM H_2O_2 for 12 h led to a significant decrease in mitochondrial ATP levels, and knockdown of Mzb1 aggravated this detrimental alteration (Fig. 4a). We then evaluated the effect of Mzb1 on mitochondrial membrane potential by confocal microscopic analysis of JC-1 staining (Fig. 4b). H_2O_2 induced depolarization of the mitochondrial membrane potential, as indicated by enhanced JC-1 staining, and this H_2O_2-induced depolarization was aggravated by si-Mzb1. We then further investigated the effect of Mzb1 on ROS production after H_2O_2 stimulation using DCFH-DA, a fluorescent

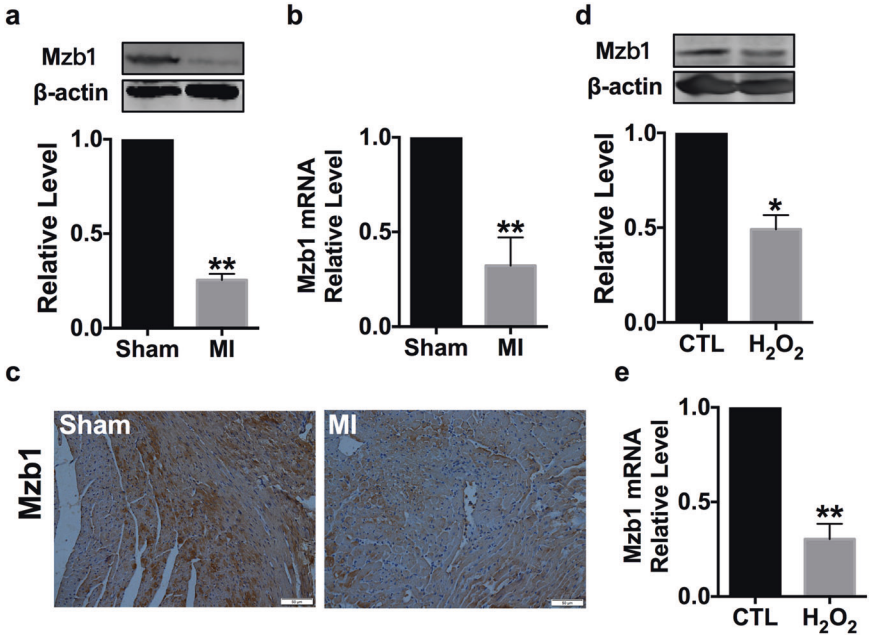

Fig. 1 Downregulation of Mzb1 expression in a mouse model of myocardial infarction (MI) and a model of oxidative stress induced by H_2O_2 in cultured neonatal mouse ventricular myocytes (NMVCs). a Downregulation of Mzb1 protein expression in MI. $n = 7$, $^{**}P < 0.01$ vs. Sham group. **b** Downregulation of Mzb1 mRNA expression in MI. $n = 4$, $^{**}P < 0.01$ vs. Sham group. **c** Representative IHC staining for Mzb1 at 24 h after ischemia (scale bar: 50 μm). **d**, **e** Expression of Mzb1 in H_2O_2-treated cardiomyocytes at the protein and mRNA levels. $n = 5$, $^{*}P < 0.05$, $^{**}P < 0.01$ vs. CTL group.

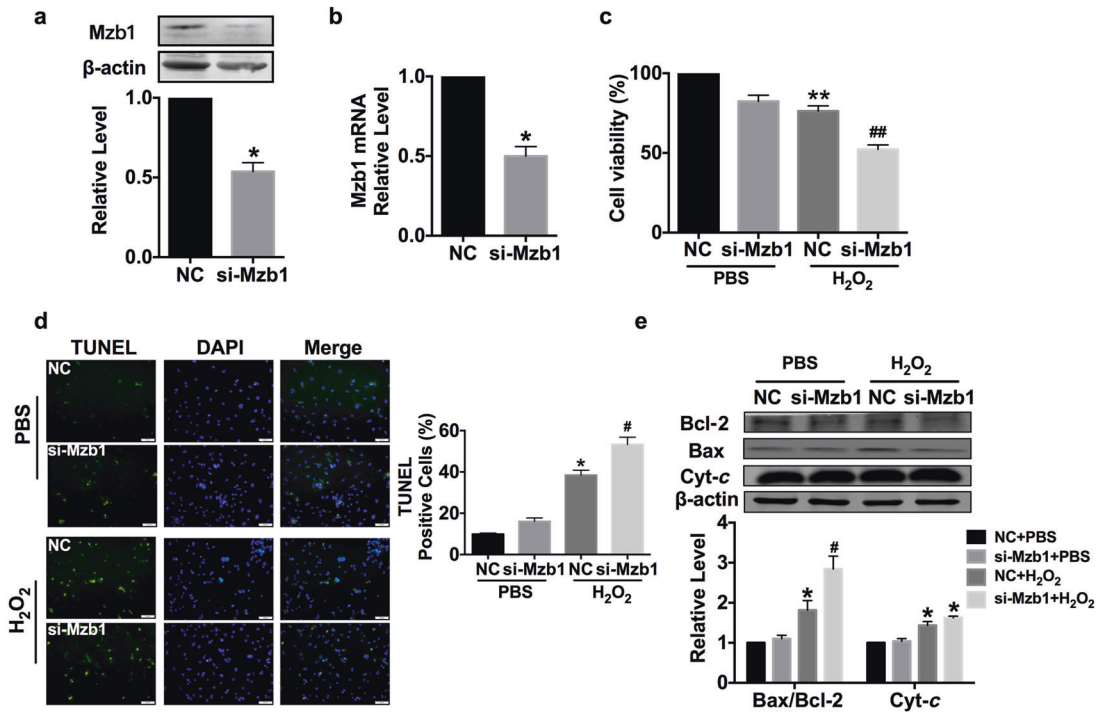

Fig. 2 Mzb1 knockdown promoted apoptosis in cardiomyocytes. a, **b** Verification of the efficacy with which si-Mzb1 silenced the expression of endogenous Mzb1 at the protein and mRNA levels in cardiomyocytes. $n = 5$, $^{*}P < 0.05$ vs. NC group. **c** Suppressive effect of silencing Mzb1 by si-Mzb1 on the viability of NMVCs in the presence of H_2O_2. Note that in the absence of H_2O_2, Mzb1 did not significantly affect cell viability. $n = 10$, $^{**}P < 0.01$ vs. NC+PBS group. $^{\#\#}P < 0.01$ vs. NC+H_2O_2 group. **d** Effects of si-Mzb1 in promoting the apoptotic cell death of NMVCs, as revealed by TUNEL staining to detect chromosome fragmentation. Left panel: representative images following TUNEL staining; right panel: averaged percentages of TUNEL-positive cells. $n = 3$, $^{*}P < 0.05$ vs. NC+PBS group, $^{\#}P < 0.05$ vs. NC+H_2O_2 group (scale bar: 50 μm). **e** Effects of si-Mzb1 on the protein levels of Bcl-2, Bax, and Cyt-*c*. $n = 5$, $^{*}P < 0.05$ vs. NC+PBS group, $^{\#}P < 0.05$ vs. NC+H_2O_2 group.

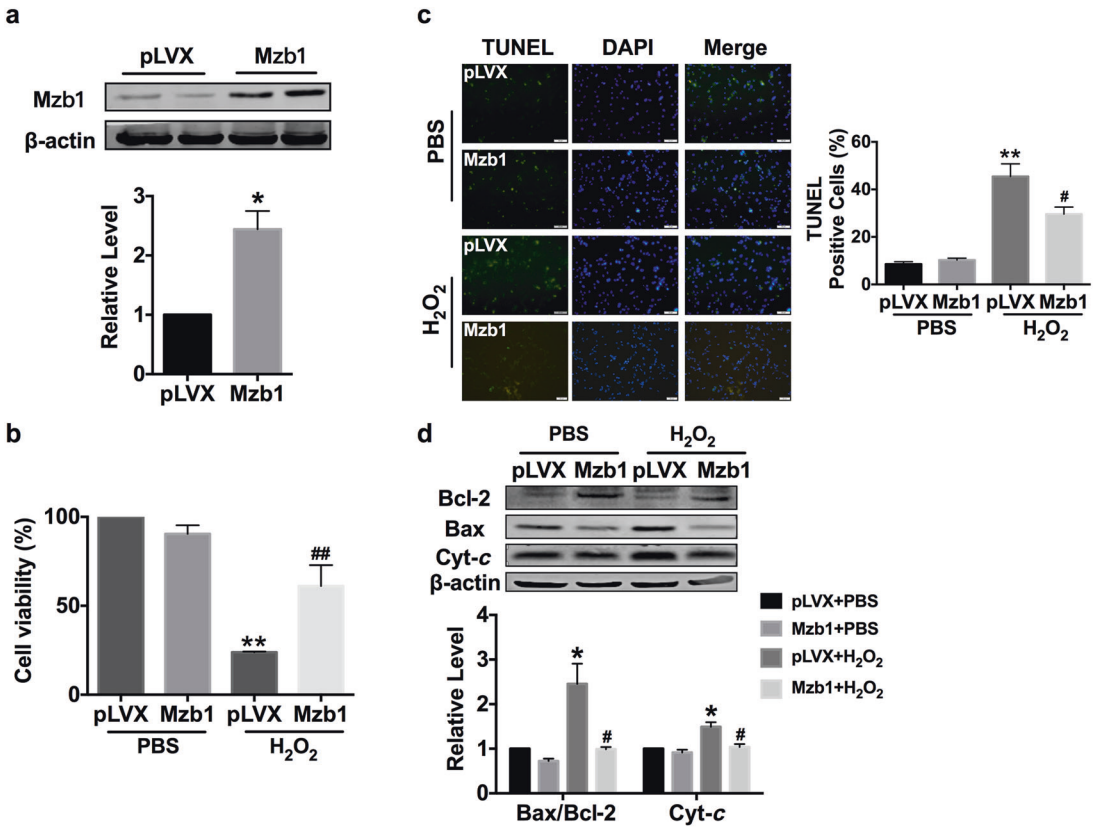

Fig. 3 Effects of Mzb1 overexpression on apoptosis in NMVCs. a Verification of Mzb1 overexpression at the protein level after infection with the pLVX plasmid containing the Mzb1 gene (Mzb1) but not the empty plasmid, which was used as a negative control (pLVX). $n = 3$, $^{*}P < 0.05$ vs. pLVX group. **b** Effect of Mzb1 overexpression in rescuing the H_2O_2-induced decrease in cell viability. $n = 7$, $^{**}P < 0.01$ vs. pLVX+PBS group. $^{\#\#}P < 0.01$ vs. pLVX + H_2O_2 group. **c** Inhibitory effects of Mzb1 overexpression on the apoptotic cell death of NMVCs, as revealed by TUNEL staining. Left panel: representative images following TUNEL staining; right panel: statistical data for the percentage of TUNEL-positive cells. $n = 3$, $^{**}P < 0.01$ vs. pLVX+PBS group, $^{\#}P < 0.05$ vs. pLVX+H_2O_2 group (scale bar: 50 μm). **d** Effect of Mzb1 on the expression of Bcl-2, Bax and Cyt-*c* at the protein level. $n = 5$, $^{*}P < 0.05$ vs. pLVX+PBS group, $^{\#}P < 0.05$ vs. pLVX+H_2O_2 group.

dye. Confocal microscopic analysis showed that the number of ROS-positive cells was markedly increased after 12 h of stimulation with H_2O_2 and that si-Mzb1 aggravated oxidative stress (Fig. 4c).

In contrast, increased Mzb1 function resulted in an increase in ATP production in the presence of H_2O_2 (Fig. 5a). Moreover, Mzb1 overexpression rescued depolarization of the mitochondrial membrane potential (Fig. 5b). As anticipated, Mzb1 overexpression mitigated the H_2O_2-induced increase in ROS-positive cells (Fig. 5c). In addition, H_2O_2 treatment significantly inhibited mitochondrial respiratory function and reduced oxygen consumption, effects that were attenuated by Mzb1 overexpression (Fig. 5d).

Mzb1 improves cardiac function and suppresses MI-induced apoptosis

Next, we continued to investigate whether the beneficial actions of Mzb1 overexpression observed in our in vitro model could be reproduced in vivo using lentivirus carrying Len-Mzb1 (Lentiviral pLVX-mCMV-ZsGreen-mMzb1*Myc) and Len-pLVX (Lentiviral pLVX-mCMV-ZsGreen). We first verified the efficiency of Len-Mzb1 transfection in inducing Mzb1 overexpression in the myocardium of mice using qRT-PCR after orthotopic injection of the virus into the myocardial tissue (Fig. 6a). We then observed that cardiac function was significantly impaired in MI mice and that overexpression of Mzb1 by Len-Mzb1 rescued this cardiac dysfunction, as indicated by increases in the EF and FS (Fig. 6b, c). Consistently, Len-Mzb1 significantly reduced the infarct size of MI mice (Fig. 6d). Moreover, MI caused a remarkable increase in the apoptosis of cardiac cells, as reflected by the increase in TUNEL-positive cells, and infection with Len-Mzb1 inhibited this increase in apoptotic cell death (Fig. 6e). The Bax/Bcl-2 ratio and Cyt-*c* expression were significantly higher in MI mice than in mice in the Sham group after infection with the negative control viral construct Len-pLVX, and these differences were abrogated by Len-Mzb1 (Fig. 6f), indicating the role of Mzb1 in repressing the expression of Bax and Cyt-*c*. Then, we investigated the ultrastructure of the infarct border zone using transmission electron microscopy (TEM) at 20,000× magnification. Electron photomicrographs of cardiomyocytes from Len-pLVX/Len-Mzb1-transfected mice in the Sham group showed a linear myofibril arrangement and normal mitochondria. After MI, Len-pLVX-transfected mice showed disoriented myofilaments and the aggregation of enlarged mitochondria. The images reveal swollen and disorganized mitochondria and fragmented mitochondria, suggesting poor respiratory capacity. However, Len-Mzb1 abolished the detrimental effects of MI, maintaining the structure and function of mitochondria (Fig. 6g). Consistent with previous reports [16], our results showed that the expression level of PGC1α and the level of phosphorylated AMPK (p-AMPK), an upstream component of PGC1α, were downregulated in MI mice, but these changes were essentially recovered by Len-Mzb1 (Fig. 6h). These results suggested that Mzb1 can affect mitochondrial function by regulating the AMPK/PGC1α signaling pathway.

Mzb1 recruits macrophages and reduces inflammation

As mitochondrial damage drives inflammation in cardiomyocytes [17], we then detected the effect of Mzb1 on the inflammatory

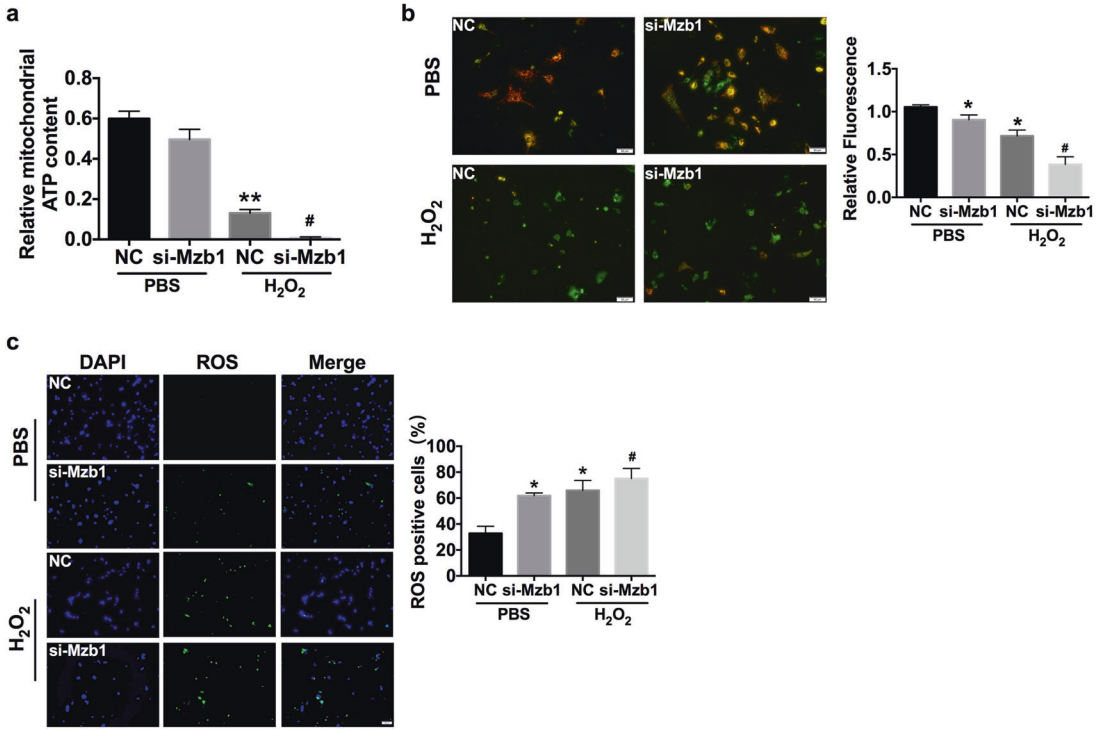

Fig. 4 Mzb1 knockdown aggravated the mitochondrial injury induced by H_2O_2. a Aggravating effects of Mzb1 silencing due to the transfection of si-Mzb1 on H_2O_2-induced depletion of the cellular ATP content in NMVCs. $n = 5$, $^{**}P < 0.01$ vs. NC+PBS group, $^{\#}P < 0.05$ vs. NC+H_2O_2 group. **b** Depolarizing effect of si-Mzb1 on mitochondrial membrane potential in NMVCs, as revealed by JC-1 staining. Left panel: representative images following JC-1 staining (scale bar: 50 μm); right panel: statistical data for the fluorescence intensities determined by JC-1 staining. JC-1 exhibits mitochondrial membrane potential-dependent accumulation in the mitochondria; in healthy cells with a high mitochondrial membrane potential, JC-1 forms a complex that emits red fluorescence, and in unhealthy cells with a low mitochondrial membrane potential, JC-1 remains in its monomeric form, emitting green fluorescence. The membrane potential is represented as the ratio of red to green fluorescence. $n = 4$, $^{*}P < 0.05$ vs. NC+PBS group, $^{\#}P < 0.05$ vs. NC+H_2O_2 group. **c** Stimulating effects of Mzb1 knockdown by si-Mzb1 on the cellular production of reactive oxygen species (ROS) in NMVCs, as detected by the ROS-specific probe DCFH-DA. Left panel: representative images following DCFH-DA fluorescence staining (scale bar: 50 μm); right panel: statistical data for the fluorescence intensities determined by DCFH-DA staining. $n = 3$, $^{*}P < 0.05$ vs. NC + PBS group, $^{\#}P < 0.05$ vs. NC+H_2O_2 group.

process in AMI. We conducted the following series of experiments. First, we demonstrated that overexpression of Mzb1 reduced release of the cytokines IL-1β, IL-6, and TNF α (Fig. 7a) as well as the NLRP3 inflammasome (Fig. 7b). As CCL2/MCP-1 is a chemokine of mononuclear macrophages [18], its expression was upregulated by Len-Mzb1 in mice in both the MI and Sham groups (Fig. 7b). We hypothesized that Mzb1 affects the accumulation of macrophages in the damaged myocardium. We then demonstrated using IHC staining that Len-Mzb1 increased the number of $CD68^{+}$ macrophages in the border zone of the infarct area of MI mice (Fig. 7c).

To confirm the recruitment of macrophages by Mzb1, we performed a Transwell assay in the mouse macrophage cell line Ana-1. The forced expression of Mzb1 promoted the migration of Ana-1 cells, whereas Mzb1 silencing by siRNA significantly inhibited their migration (Fig. 7d). We further tested the autonomous migration ability of the cells by using a wound-healing assay. As shown in Fig. 7e, Mzb1 significantly reduced the wounded area in the Ana-1 cells, while si-Mzb1 did not affect the wound-healing process. In addition, Mzb1 overexpression promoted cell proliferation, whereas the silencing of endogenous Mzb1 failed to alter it (Fig. 7f).

DISCUSSION

Here, we characterized for the first time the cardioprotective property of Mzb1. First, the expression of Mzb1 was found to be considerably decreased in a mouse model of MI and in H_2O_2-treated cardiomyocytes in vitro. This downregulation of Mzb1 contributed to the MI-induced impairment of cardiac function in vivo and promoted cardiomyocyte apoptosis induced by H_2O_2 in vitro. In contrast, overexpression of Mzb1 improved cardiac function and alleviated H_2O_2-induced cardiomyocyte apoptosis. Furthermore, we demonstrated that Mzb1 markedly improved mitochondrial function in H_2O_2-treated cardiomyocytes with the restoration of decreased mitochondrial ATP synthesis and mitochondrial respiratory function and reduced production of ROS. Mzb1 overexpression regulated the AMPK/PGC1α signaling pathway. In addition, Mzb1 recruited macrophages and inhibited inflammation in MI. We therefore conclude that Mzb1 protects against MI injury by modulating mitochondrial function and reducing inflammation in mouse cardiomyocytes (Fig. 8).

Cardiovascular disease is a major human health issue that causes serious damage to human life and health [19]. Population aging increases the incidence of multifarious cardiovascular diseases, including MI. Although the development and maturation of coronary artery intervention, coronary artery bypass graft surgery, and other treatment techniques have greatly improved the rates of cardiovascular disease diagnosis and treatment and significantly decreased the mortality of patients with AMI, we should still focus on exploring MI. Our in vitro and in vivo results indicate that Mzb1 overexpression improved cardiac function in MI mice, restored the decreased cell viability induced by H_2O_2, and reduced apoptotic cell death.

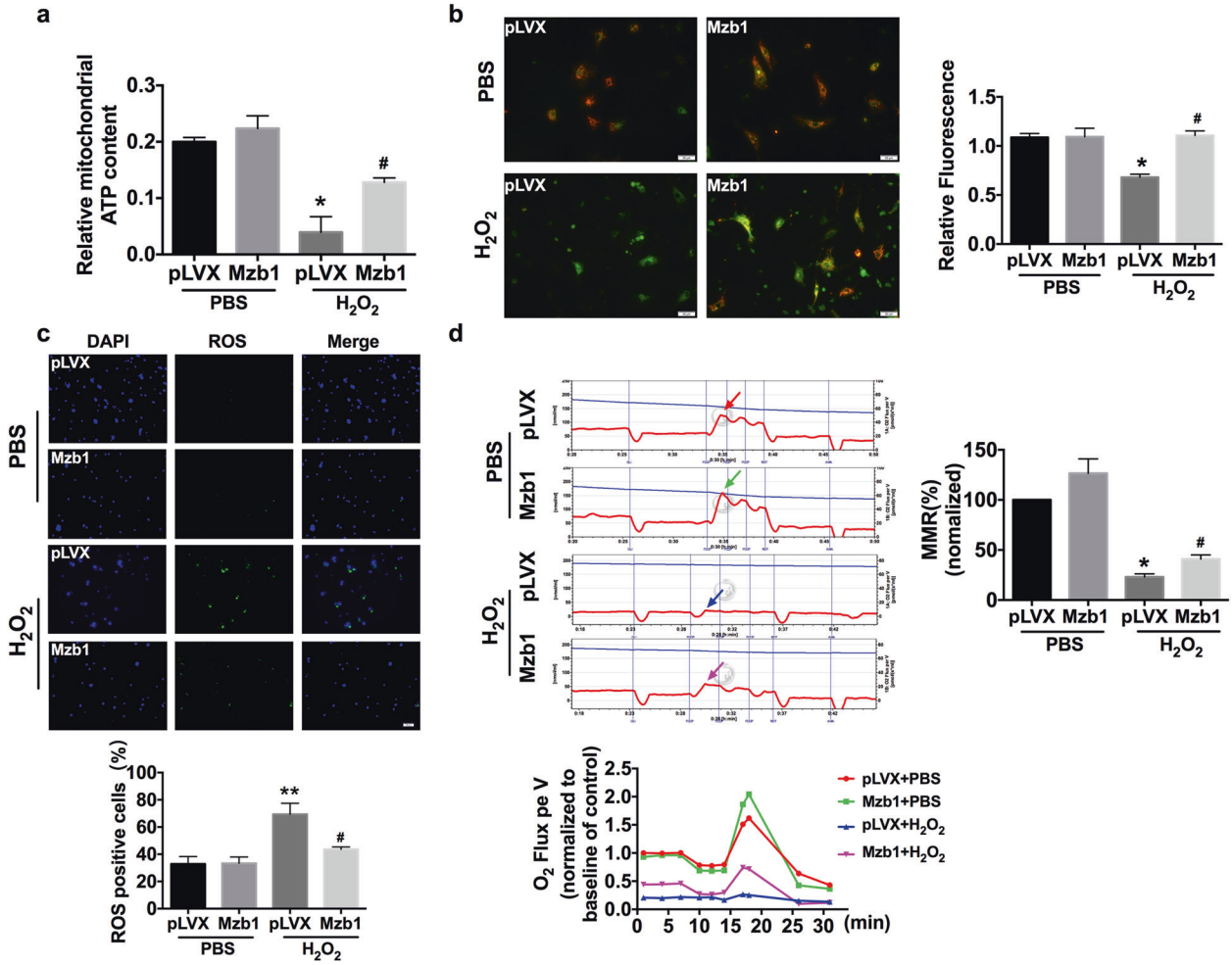

Fig. 5 Mzb1 overexpression significantly improves mitochondrial function. a Mzb1 overexpression after transfection of Mzb1 elevated the cellular ATP content in NMVCs treated with H_2O_2. $n = 6$, $^*P < 0.05$ vs. pLVX+PBS group, $^{\#}P < 0.05$ vs. pLVX+H_2O_2 group. **b** Mzb1 overexpression rescued H_2O_2-induced depolarization of the mitochondrial membrane potential in NMVCs, as revealed by JC-1 staining. Left panel: representative images following JC-1 staining (scale bar: 50 μm); right panel: statistical data for the fluorescence intensities determined by JC-1 staining. JC-1 exhibits mitochondrial membrane potential-dependent accumulation in the mitochondria; in healthy cells with a high mitochondrial membrane potential, JC-1 forms a complex that emits red fluorescence, and in unhealthy cells with a low mitochondrial membrane potential, JC-1 remains in its monomeric form, emitting green fluorescence. The membrane potential is represented by the ratio of red to green fluorescence. $n = 4$, $^*P < 0.05$ vs. pLVX+PBS group, $^{\#}P < 0.05$ vs. pLVX+H_2O_2 group. **c** Mzb1 overexpression suppressed the cellular production of ROS in NMVCs, as detected by DCFH-DA fluorescence staining. Upper panel: representative images following DCFH-DA staining (scale bar: 50 μm); lower panel: statistical data for the fluorescence intensities determined by DCFH-DA staining. $n = 3$, $^{**}P < 0.01$ vs. pLVX+PBS group, $^{\#}P < 0.05$ vs. pLVX+H_2O_2 group. **d** Representative profiles and summarized data regarding oxygen consumption in cardiomyocytes. The blue line indicates the oxygen concentration in the detection chamber. The red line indicates oxygen consumption per unit volume and per unit time detected in real-time, MMR: maximal mitochondrial respiration. $n = 3$, $^*P < 0.05$ vs. pLVX +PBS group, $^{\#}P < 0.05$ vs. pLVX +H_2O_2 group.

Mzb1, a B-cell-specific and endoplasmic reticulum (ER)-localized protein, is one of the key factors affecting immune protein synthesis. As a target of Mzb1, microRNA-185 causes developmental arrest of T cells [20]. Mzb1 also affects the maturation of immune cells [21]. In previous reports, researchers focused on the function of Mzb1 in endoplasmic reticulum stress and immune inflammation. ER stress has been linked to both physiological and pathological states in the cardiovascular system, including MI [22]. Thus, we raised the question of whether Mzb1 participates in ER stress during AMI. By detecting the ER stress chaperones GRP94 and GRP78, we found that they could interact with Mzb1 (results not shown) and that Mzb1 could limit the expression of GRP94 and GRP78. This prompted us to propose that Mzb1 is involved in ER stress in MI and affects the classical signal pathway of ER stress.

Recent studies have revealed the remarkable complexity of mitochondrial protein organization [23, 24]. Protein machinery with diverse functions, such as protein translocation, respiration, metabolite transport [25], protein quality control [26], and the control of membrane architecture interact in dynamic networks [27]. Mzb1 affects some immune protein synthesis, which raised the question of whether there is a necessary relationship between Mzb1 and mitochondria. Mitochondria and ER are interconnected organelles, and contact points where the ER communicates with mitochondria are referred to as mitochondria-associated ER membranes (MAMs) [28, 29]. Using a mitochondrial protein extraction kit, we found that Mzb1 may also localize to mitochondria. While our study is limited by some factors, we would like to determine whether Mzb1 is present on MAMs. Another limitation of our study is that to create transgenic mice with Mzb1 knockdown, we hybridized heterozygous $Mzb^{-/+}$ mice to generate homozygous $Mzb^{-/-}$ mice, among which the natality was very low, and most neonatal mice were male. We concluded

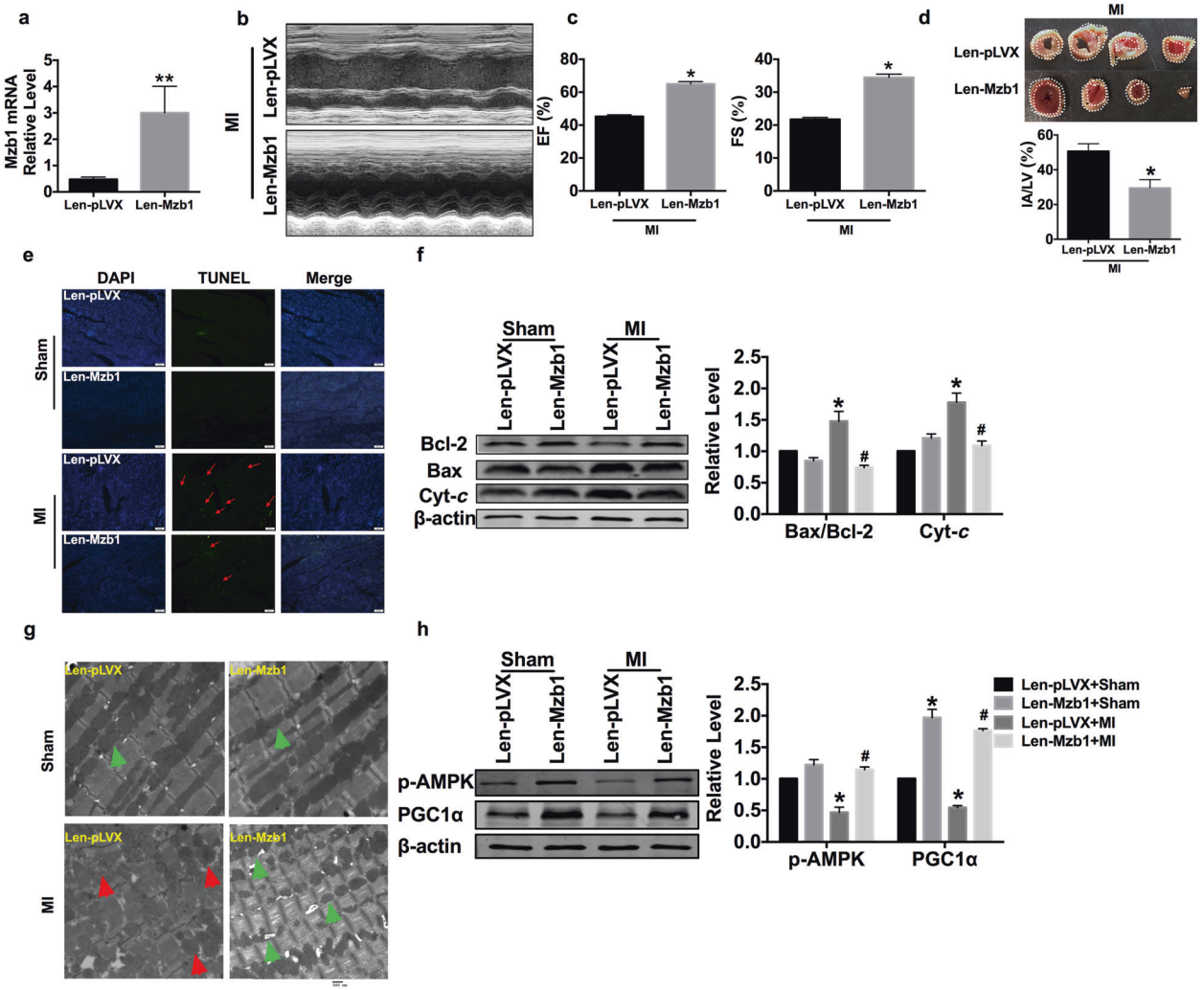

Fig. 6 Mzb1 overexpression suppresses cardiomyocyte apoptosis in MI mice. a Verification of Mzb1 overexpression one week after direct injection of lentivirus expressing Mzb1 (Len-Mzb1) into the myocardium using real-time RT-PCR. $n = 5$, $^{**}P < 0.01$ vs. Len-pLVX group. **b** Cardiac parameters of the mouse model were detected by M-mode echocardiography. **c** Echocardiographic analysis showing the ability of Mzb1 overexpression by Len-Mzb1 to reverse the decreased left ventricular ejection fraction (EF) and left ventricular fractional shortening (FS) in MI mice. $n = 6$, $^{*}P < 0.05$ vs. Len-pLVX+MI group. **d** TTC staining exhibiting the efficacy with which Len-Mzb1 transfection reduced the infarct size of MI mice. Upper panel: representative TTC staining of heart sections from Len-pLVX- and Len-Mzb1-treated MI mice; lower panel: mean data for the percentage of the infarct area over the total area. $n = 6$, $^{*}P < 0.05$ vs. Len-pLVX+MI group. **e** The anti-apoptotic effect of Len-Mzb1 was revealed by TUNEL staining. **f** Effect of Len-Mzb1 on the protein levels of Bcl-2, Bax and Cyt-*c*. $n = 6$, $^{*}P < 0.05$ vs. Len-pLVX+Sham group, $^{\#}P < 0.05$ vs. Len-pLVX+MI group. **g** Electron microscopic findings of the myocardial ultrastructure. The red arrow indicates swollen and disorganized mitochondria and fragmented mitochondria. The green arrow indicates normal mitochondrial ultrastructure. Original magnification, ×20,000; scale bar = 500 nm. **h** Effect of Len-Mzb1 on the protein levels of p-AMPK and PGC1α. $n = 6$, $^{*}P < 0.05$ vs. Len-pLVX+Sham group, $^{\#}P < 0.05$ vs. Len-pLVX+MI group.

that Mzb1 may affect embryonic development, especially processes controlled by the X chromosome. We may solve this problem by creating conditional knockout mice.

Damage caused by free radical-induced oxidation in humans is thought to play a significant role in ischemic disease and contribute to the development of disease [30]. During myocardial infarction, many oxygen free radicals are produced in cardiomyocytes, which cause injury to mitochondrial function. Based on the mitochondrial localization of Mzb1, we determined the effects of Mzb1 on mitochondrial function [31]. Our study showed that Mzb1 increased mitochondrial ATP production and oxygen consumption in H_2O_2-induced cardiomyocytes. Mzb1 also significantly reduced the synthesis of mitochondrial ROS. Most studies have shown that PGC1α is an important regulator of energetic metabolism for cardiac growth under various physiological and pathological stimuli [32]. Tangeretin enhanced mitochondrial biogenesis by activating the AMPK-PGC1α pathway, resulting in improved exercise performance [33]. We found that Mzb1 may modulate mitochondrial function by regulating the AMPK-PGC1α pathway.

In response to external stimuli, the release of endogenous molecules containing damage-associated molecular patterns (DAMPs) triggers an inflammatory response in the heart. The NLRP3 inflammasome activation is increasingly recognized as an important mechanism linking mitochondrial function and integrity to innate immunity. Increased mitochondrial damage associated with increased oxidative stress contributes to cardiac inflammation [17]. Here, we observed a decreased level of NLRP3 in mice with forced Mzb1 expression. Furthermore, our results showed that Mzb1 affected the expression of mononuclear macrophage

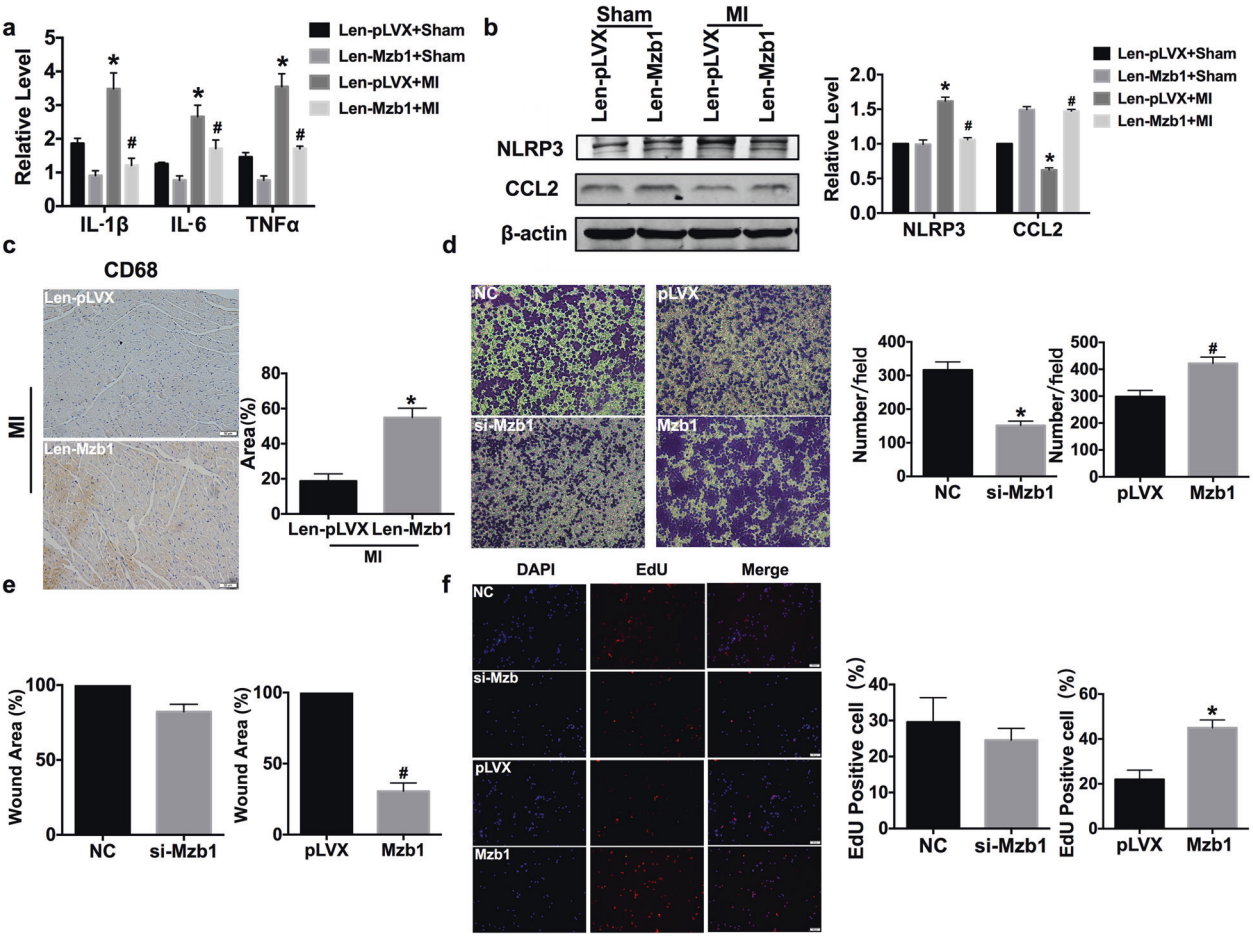

Fig. 7 Mzb1 reduces inflammation and accumulates macrophages in MI mice. a The mRNA expression of inflammatory factors (IL-1β, IL-6, and TNFα). $n = 5$, $^{*}P < 0.05$ vs. Len-pLVX+Sham group, $^{\#}P < 0.05$ vs. Len-pLVX+MI group. **b** Representative Western blot bands consisting of NLRP3 and CCL2 in different groups. $n = 6$, $^{*}P < 0.05$ vs. Len-pLVX+Sham group, $^{\#}P < 0.05$ vs. Len-pLVX+MI group. **c** Representative IHC staining for CD68 after myocardial injection with Mzb1 plasmid in MI mice (scale bar: 50 μm). $n = 4$, $^{*}P < 0.05$ vs. Len-pLVX+MI group. **d** Representative images showing the migration of Ana-1 cells in the Transwell assays. Cell counts are for the corresponding assays in at least four random microscope fields (×100 magnification). $n = 4$, $^{*}P < 0.05$ vs. NC group, $^{\#}P < 0.05$ vs. pLVX group. **e** Results of the wound-healing assay in Ana-1 cells with Mzb1 overexpression and silencing are quantified in the histogram. $n = 6$, $^{\#}P < 0.05$ vs. pLVX group. **f** Representative images showing the proliferation of Ana-1 cells in the EdU assay. $n = 6$, $^{*}P < 0.05$ vs. pLVX group.

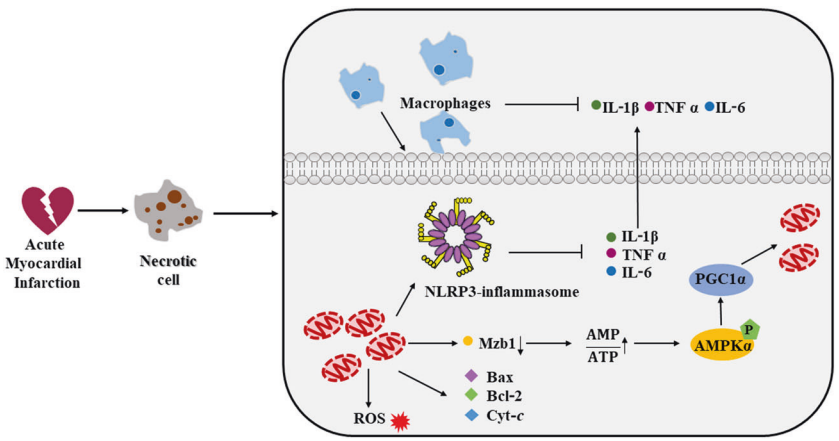

Fig. 8 Schematic model describing the protective effect of Mzb1 in AMI. Injury of cardiomyocytes led to apoptosis and mitochondrial dysfunction, ROS release, and increased inflammation. Mzb1 prevented injury through AMPK-PGC1α signaling pathway, recruited macrophages, and inhibited the release of inflammatory cytokines, which recovered mitochondrial function and decreased inflammation in mouse cardiomyocytes.

CCL2, and we then explored the link between Mzb1 and macrophage infiltration. Through our research, we demonstrated that Mzb1 promotes macrophage proliferation and migration. If possible, we will next detect the effect of Mzb1 on macrophage accumulation.

In conclusion, the results of this study suggest that Mzb1 protects cardiomyocytes in myocardial infarction by regulating mitochondrial function and reducing inflammation. This discovery provides new targets and intervention means for the treatment of disordered mitochondrial energetic metabolism in myocardial infarction.

ACKNOWLEDGEMENTS

This study was supported by the National Natural Science Foundation of China (81770284, 31671187, 81673425), and the CAMS Innovation Fund for Medical Sciences (CIFMS, 2019-I2M-5-078).

AUTHOR CONTRIBUTIONS

HHL and BFY designed and supervised all aspects of the study and analysis. LZ, YNW, JMJ, AS, YL, and TYL performed study and analysis the data. RNF, JBS, YYG, TZJ, and YYL assisted in this study. HLS, HHL, and BFY finalized the manuscript.

ADDITIONAL INFORMATION

Competing interests: The authors declare no competing interests.

REFERENCES

1. Elgendy IY, Mahtta D, Pepine CJ. Medical therapy for heart failure caused by ischemic heart disease. Circ Res. 2019;124:1520–35.
2. Maneechote C, Palee S, Chattipakorn SC, Chattipakorn N. Roles of mitochondrial dynamics modulators in cardiac ischaemia/reperfusion injury. J Cell Mol Med. 2017;21:2643–53.
3. Frankenreiter S, Bednarczyk P, Kniess A, Bork NI, Straubinger J, Koprowski P, et al. cGMP-elevating compounds and ischemic conditioning provide cardioprotection against ischemia and reperfusion injury via cardiomyocyte-specific BK channels. Circulation. 2017;136:2337–55.
4. Ruparelia N, Chai JT, Fisher EA, Choudhury RP. Inflammatory processes in cardiovascular disease: a route to targeted therapies. Nat Rev Cardiol. 2017;14:133–44.
5. Rawat P, Teodorof-Diedrich C, Spector SA. Human immunodeficiency virus Type-1 single-stranded RNA activates the NLRP3 inflammasome and impairs autophagic clearance of damaged mitochondria in human microglia. Glia. 2019;67:802–24.
6. Rosenbaum M, Andreani V, Kapoor T, Herp S, Flach H, Duchniewicz M, et al. MZB1 is a GRP94 cochaperone that enables proper immunoglobulin heavy chain biosynthesis upon ER stress. Genes Dev. 2014;28:1165–78.
7. Andreani V, Ramamoorthy S, Pandey A, Lupar E, Nutt SL, Lammermann T, et al. Cochaperone Mzb1 is a key effector of Blimp1 in plasma cell differentiation and beta1-integrin function. Proc Natl Acad Sci USA. 2018;115:E9630–9.
8. Miyagawa-Hayashino A, Yoshifuji H, Kitagori K, Ito S, Oku T, Hirayama Y, et al. Increase of MZB1 in B cells in systemic lupus erythematosus: proteomic analysis of biopsied lymph nodes. Arthritis Res Ther. 2018;20:13.
9. Zhang Y, Wang Y, Xu J, Tian F, Hu S, Chen Y, et al. Melatonin attenuates myocardial ischemia-reperfusion injury via improving mitochondrial fusion/mitophagy and activating the AMPK-OPA1 signaling pathways. J Pineal Res. 2019;66:e12542.
10. Yang B, Lin H, Xiao J, Lu Y, Luo X, Li B, et al. The muscle-specific microRNA miR-1 regulates cardiac arrhythmogenic potential by targeting GJA1 and KCNJ2. Nat Med. 2007;13:486–91.
11. Li C, Li X, Gao X, Zhang R, Zhang Y, Liang H, et al. MicroRNA-328 as a regulator of cardiac hypertrophy. Int J Cardiol. 2014;173:268–76.
12. Tai Y, Li L, Peng X, Zhu J, Mao X, Qin N, et al. Mitochondrial uncoupler BAM15 inhibits artery constriction and potently activates AMPK in vascular smooth muscle cells. Acta Pharm Sin B. 2018;8:909–18.
13. Zhou H, Zhu P, Wang J, Zhu H, Ren J, Chen Y. Pathogenesis of cardiac ischemia reperfusion injury is associated with CK2alpha-disturbed mitochondrial homeostasis via suppression of FUNDC1-related mitophagy. Cell Death Differ. 2018;25:1080–93.
14. Kentner R, Safar P, Behringer W, Wu X, Kagan VE, Tyurina YY, et al. Early antioxidant therapy with Tempol during hemorrhagic shock increases survival in rats. J Trauma. 2002;53:968–77.
15. Penna C, Perrelli MG, Pagliaro P. Mitochondrial pathways, permeability transition pore, and redox signaling in cardioprotection: therapeutic implications. Antioxid Redox Signal. 2013;18:556–99.
16. Canto C, Auwerx J. PGC-1alpha, SIRT1 and AMPK, an energy sensing network that controls energy expenditure. Curr Opin Lipido. 2009;20:98–105.
17. Mills EL, Kelly B, O'Neill LAJ. Mitochondria are the powerhouses of immunity. Nat Immunol. 2017;18:488–98.
18. Kwon MJ, Shin HY, Cui Y, Kim H, Thi AH, Choi JY, et al. CCL2 Mediates neuron-macrophage interactions to drive proregenerative macrophage activation following preconditioning injury. J Neurosci. 2015;35:15934–47.
19. Lee PL, Jung SM, Guertin DA. The complex roles of mechanistic target of rapamycin in adipocytes and beyond. Trends Endocrinol Metab. 2017;28:319–39.
20. Belkaya S, Murray SE, Eitson JL, de la Morena MT, Forman JA, van Oers NS. Transgenic expression of microRNA-185 causes a developmental arrest of T cells by targeting multiple genes including Mzb1. J Biol Chem. 2013;288:30752–62.
21. Flach H, Rosenbaum M, Duchniewicz M, Kim S, Zhang SL, Cahalan MD, et al. Mzb1 protein regulates calcium homeostasis, antibody secretion, and integrin activation in innate-like B cells. Immunity. 2010;33:723–35.
22. Groenendyk J, Agellon LB, Michalak M. Coping with endoplasmic reticulum stress in the cardiovascular system. Annu Rev Physiol. 2013;75:49–67.
23. Xu T, Ding W, Ao X, Chu X, Wan Q, Wang Y, et al. ARC regulates programmed necrosis and myocardial ischemia/reperfusion injury through the inhibition of mPTP opening. Redox Biol. 2019;20:414–26.
24. Cooper HA, Eguchi S. Inhibition of mitochondrial fission as a novel therapeutic strategy to reduce mortality upon myocardial infarction. Clin Sci (Lond). 2018;132:2163–7.
25. Thoudam T, Ha CM, Leem J, Chanda D, Park JS, Kim HJ, et al. PDK4 augments ER-mitochondria contact to dampen skeletal muscle insulin signaling during obesity. Diabetes. 2019;68:571–86.
26. Wu S, Lu Q, Ding Y, Wu Y, Qiu Y, Wang P, et al. Hyperglycemia-driven inhibition of AMP-activated protein kinase alpha2 induces diabetic cardiomyopathy by promoting mitochondria-associated endoplasmic reticulum membranes in vivo. Circulation. 2019;139:1913–36.
27. Pfanner N, Warscheid B, Wiedemann N. Mitochondrial proteins: from biogenesis to functional networks. Nat Rev Mol Cell Biol. 2019;20:267–84.
28. Rowland AA, Voeltz GK. Endoplasmic reticulum-mitochondria contacts: function of the junction. Nat Rev Mol Cell Biol. 2012;13:607–25.
29. Wu S, Lu Q, Wang Q, Ding Y, Ma Z, Mao X, et al. Binding of FUN14 domain containing 1 with inositol 1,4,5-trisphosphate receptor in mitochondria-associated endoplasmic reticulum membranes maintains mitochondrial dynamics and function in hearts in vivo. Circulation. 2017;136:2248–66.
30. Li Q, Tursun D, Shi C, Heyrulla M, Zhang X, Yang W. Ziziphora clinopodioides flavonoids protect myocardial cell damage from myocardial ischemia-reperfusion injury. Evid Based Complement Altern Med. 2018;2018:8495010.
31. Yang J, He J, Ismail M, Tweeten S, Zeng F, Gao L, et al. HDAC inhibition induces autophagy and mitochondrial biogenesis to maintain mitochondrial homeostasis during cardiac ischemia/reperfusion injury. J Mol Cell Cardiol. 2019;130:36–48.
32. Butterick TA, Hocum Stone L, Duffy C, Holley C, Cabrera JA, Crampton M, et al. Pioglitazone increases PGC1-alpha signaling within chronically ischemic myocardium. Basic Res Cardiol. 2016;111:37. https://doi.org/10.1007/s00395-016-0555-4.
33. Kou G, Li Z, Wu C, Liu Y, Hu Y, Guo L, et al. Citrus tangeretin improves skeletal muscle mitochondrial biogenesis via activating the AMPK-PGC1-alpha pathway in vitro and in vivo: a possible mechanism for its beneficial effect on physical performance. J Agric Food Chem. 2018;66:11917–25.